



Published in final edited form as:

Nature. 2013 October 3; 502(7469): 100–104. doi:10.1038/nature12519.

Immune clearance of highly pathogenic SIV infection

Scott G. Hansen^{1,*}, Michael Piatak Jr.^{2,*}, Abigail B. Ventura¹, Colette M. Hughes¹, Roxanne M. Gilbride¹, Julia C. Ford¹, Kelli Oswald², Rebecca Shoemaker², Yuan Li², Matthew S. Lewis¹, Awbrey N. Gilliam¹, Guangwu Xu¹, Nathan Whizin¹, Benjamin J. Burwitz¹, Shannon L. Planer¹, John M. Turner¹, Alfred W. Legasse¹, Michael K. Axthelm¹, Jay A. Nelson¹, Klaus Früh¹, Jonah B. Sacha¹, Jacob D. Estes², Brandon F. Keele^{2,3}, Paul T. Edlefsen³, Jeffrey D. Lifson², and Louis J. Picker¹

¹Vaccine and Gene Therapy Institute and Oregon National Primate Research Center, Oregon Health & Science University, Beaverton, OR 97006

²AIDS and Cancer Virus Program, SAIC Frederick, Inc., Frederick National Laboratory, Frederick, MD 21702

³Statistical Center for HIV/AIDS Research and Prevention, Vaccine and Infectious Disease Division, Fred Hutchinson Cancer Research Center, Seattle, WA 98109

Abstract

Established infections with the human and simian immunodeficiency viruses (HIV, SIV) are thought to be permanent with even the most effective immune responses and anti-retroviral therapies (ART) only able to control, but not clear, these infections^{1–4}. Whether the residual virus that maintains these infections is vulnerable to clearance is a question of central importance to the future management of millions of HIV-infected individuals. We recently reported that ~50% of rhesus macaques (RM) vaccinated with SIV protein-expressing Rhesus Cytomegalovirus (RhCMV/SIV) vectors manifest durable, aviremic control of infection with highly pathogenic SIVmac239⁵. Here, we demonstrate that regardless of route of challenge, RhCMV/SIV vector-elicited immune responses control SIVmac239 after demonstrable lymphatic and hematogenous viral dissemination, and that replication-competent SIV persists in multiple sites for weeks to months. However, over time, protected RM lost signs of SIV infection, showing a consistent lack of measurable plasma or tissue-associated virus using ultrasensitive assays, and loss of T cell

Users may view, print, copy, download and text and data- mine the content in such documents, for the purposes of academic research, subject always to the full Conditions of use: http://www.nature.com/authors/editorial_policies/license.html#terms

Correspondence and request for materials should be addressed to either JDL lifsonj@mail.nih.gov or LJP (pickerl@ohsu.edu).

*These authors contributed equally to this work.

AUTHOR CONTRIBUTIONS: SGH planned and performed animal experiments and analyzed immunologic and virologic data, assisted by ABV, CMH, RMG, JCF, MSL, ANG, GX and NW. MP, Jr. and JDL planned and performed SIV quantification, assisted by KO, RS and YL. BJB and JBS performed infected cell recognition assays. BFK performed sequencing analysis. JDE performed immunohistologic studies. SLP, JMT, AWL and MKA managed the animal protocols. JAN and KF supervised CMV vector design and development. JDL planned and supervised SIV quantification and immunohistologic experiments. PTE performed all statistical analyses. LJP conceived the RhCMV vector strategy, supervised all experiments, analyzed data, and wrote the paper, assisted by SGH, JDL and JBS.

New SIVmac239 sequences reported in this manuscript are accessible in Genbank (accession #s KF439057, KF439058, KF439059).

The authors declare the following competing financial interests: OHSU and Drs. Picker, Hansen, Früh and Nelson have a significant financial interest in TomegaVax, Inc., a company that may have a commercial interest in the results of this research and technology. The potential individual and institutional conflicts of interest have been reviewed and managed by OHSU.

reactivity to SIV determinants not in the vaccine. Extensive ultrasensitive RT-PCR and PCR analysis of tissues from RhCMV/SIV vector-protected RM necropsied 69–172 weeks after challenge did not detect SIV RNA or DNA over background, and replication-competent SIV was not detected in these RM by extensive co-culture analysis of tissues or by adoptive transfer of 60 million hematolymphoid cells to naïve RM. These data provide compelling evidence for progressive clearance of a pathogenic lentiviral infection, and suggest that some lentiviral reservoirs may be susceptible to the continuous effector memory T cell-mediated immune surveillance elicited and maintained by CMV vectors.

Both clinical and experimental observations have suggested that HIV/SIV infections might be vulnerable to immune control or pharmacologic clearance in the first hours to days of infection, prior to the viral amplification needed for efficient immune evasion and to the establishment of the highly resilient viral reservoir that sustains the infection^{4,6–8}. CMV vectors were designed to exploit this putative window of vulnerability based on their ability to elicit and indefinitely maintain high frequency, effector-differentiated, and broadly targeted virus-specific T cells in potential sites of early viral replication^{5,9,10}. Indeed, the pattern of protection observed in ~50% of RhCMV/SIV vector-vaccinated RM after intra-rectal (IR) SIVmac239 challenge was consistent with early immunologic interception of the nascent SIV infection at the portal of viral entry and immune control prior to irreversible systemic spread⁵. Protected RM manifested a very transient viremia at the onset of infection followed by control of plasma SIV levels to below the threshold of quantification, except for occasional plasma viral “blips” that waned over time, and after one year, demonstrated only trace levels of tissue-associated SIV RNA and DNA at necropsy using ultrasensitive assays. The occurrence of plasma viral blips and the recurrence of “breakthrough” progressive infection in 1 of the 13 RhCMV/SIV vector-protected RM at day 77 post-infection indicated that SIV was not immediately cleared, but the failure to find more than trace levels of SIV nucleic acid in systemic lymphoid tissues was consistent with the productive infection being largely contained in the portal of entry with the possibility of eventual clearance. Given the critical importance of understanding the degree to which a highly pathogenic lentivirus can be contained or even cleared by adaptive immunity, we sought to more precisely define the spread and dynamics of SIV infection in RM that controlled the infection as a consequence of RhCMV/SIV vector vaccination, and in particular, the extent to which residual SIV was eventually cleared from these animals.

To establish the extent of SIV spread early after the onset of RhCMV/SIV vector-mediated control, we studied a group of 5 RM vaccinated with RhCMV vectors containing SIVgag, rev/tat/nef (rtn), env and pol (but not vif) inserts that were taken to necropsy within 24 days of controlling plasma viremia after IR inoculation with SIVmac239. All of these RM had measureable SIV RNA in plasma for 1 or 2 weekly time points after challenge followed by at least 3 consecutive weekly samples with plasma SIV RNA below 30 copy equivalents (c. eq.) per ml, and at the time of necropsy, below 5 c. eq./ml, as measured by an ultrasensitive assay (Fig. 1a). Infection was confirmed by the *de novo* development of T cell responses against SIVvif (not included in the vaccine) in all RM (Fig. 1b; Suppl. Fig. 1a). As previously described⁵, protection occurred without anamnestic boosting of vaccine-elicited SIV-specific CD8+ T cell responses in blood (Fig. 1b), and at necropsy, robust CD4+ and

CD8⁺ T cell responses to the SIV proteins included in the RhCMV/SIV vaccine vectors were identified (Suppl. Fig. 1b). We then used ultrasensitive, nested PCR and RT-PCR assays to quantify SIV DNA and RNA, respectively, in the tissues of these protected RM, in comparison with tissues from 3 unchallenged, RhCMV/SIV vector-vaccinated RM (SIV–controls), 2 unvaccinated RM with productive SIV infection (1 progressor and 1 elite controller) and 3 RM with SIV infection suppressed with ART (Fig. 1c; Suppl. Figs. 2–4; Suppl. Table 1). Two of the 5 RhCMV/SIV vector-protected RM showed levels of SIV DNA and RNA approaching the very low level background signal observed for SIV–control RM. However, the other 3 showed readily measurable SIV RNA, not only in rectal/colonic mucosa (portal of entry), but also in lymph nodes (LNs) draining the portal of entry (iliosacral and mesenteric), as well as sites of presumed hematogenous spread: bone marrow (BM), spleen, and liver. The level of SIV RNA in the tissues of these RM was less than that seen in progressive infection, but comparable to that in the elite SIV controller and in ART-suppressed SIV infection. Notably, however, levels of tissue-associated SIV DNA in the RhCMV/SIV vector-protected RM were all substantially lower than in the RM with elite control and ART suppression, most likely reflecting virologic control before, rather than after, peak viral replication in the RhCMV/SIV vector-protected RM, and the limited time for SIV DNA⁺ cells to accumulate in these RM prior to necropsy. While these data suggest a much smaller SIV reservoir in the RhCMV/SIV vector-protected RM compared to the SIV + controls, including ART-suppressed infected RM, we were able to recover replication-competent SIV from iliosacral LNs and spleen in all 5 of the RhCMV/SIV-protected RM taken to early necropsy (and from BM and mesenteric LNs in 3 of 5 of these RM), including the 2 RM with near background levels of SIV RNA by nested RT-PCR (Table 1). This replication-competent SIV was found in tissues manifesting only minimal interferon-stimulated gene expression, significantly less than found in either progressive or ART-suppressed SIV infection (Suppl. Fig. 5). Taken together, these data demonstrate that in RhCMV/SIV vector-protected RM, SIV can escape the portal of entry and establish infection in draining LNs, as well as BM, spleen and liver, prior to stringent control.

Following IR inoculation, SIV infection has been reported to spread to draining LNs within 4 hours¹¹, a rate of dissemination that may preclude SIV-specific effector memory T cells from containing the infection within the mucosa. In contrast, the development of SIV infection after intra-vaginal (IVag) inoculation has been reported to require local amplification, with distal spread only after 4–5 days⁶. To determine whether RhCMV/SIV vector-elicited T cell responses might locally control and perhaps clear an IVag SIV challenge, we compared the outcome of repeated, limiting dose IVag SIVmac239 challenge in cycling female RM vaccinated twice (week 0 and 14) with RhCMV/SIV vectors (Group A) vs. similar RM vaccinated twice with RhCMV vectors encoding non-SIV inserts (Group B) or left unvaccinated (Group C) with challenge 78 weeks after initial vaccination (Suppl. Fig. 6). The immunogenicity of RhCMV/SIV vectors in these female RM was similar to that described for male RM with robust, effector memory-biased SIV-specific CD4⁺ and CD8⁺ T cell responses to all SIV inserts (Suppl. Figs. 7, 8), but little to no SIVenv-specific antibody responses (Suppl. Fig. 9). As previously described for IR challenge of male RM⁵, RhCMV/SIV vector vaccination did not significantly affect the number of challenges required to achieve infection relative to control-vaccinated and unvaccinated RM (Suppl.

Fig. 10), but did dramatically alter the course of infection with 9 of 16 RhCMV/SIV vector-vaccinated female RM manifesting stringent (MHC class I allele-independent) control of plasma viremia compared with none of 18 infected female control RM (Fig. 2a; Suppl. Table 2). Five of these 9 protected female RM manifested a second episode of transient plasma viremia within the first 12 weeks after initial control, but overall, the fraction of RM (followed for at least 30 weeks) with such plasma viral blips (56% vs. 100%; $p = 0.02$ by Fisher's exact test) and the number of blips per RM (0.7 vs. 6.0; $p < 0.0001$ by two-sided Wilcoxon Rank Sum test) were less than observed in RhCMV/SIV vector-vaccinated male RM protected after IR challenge⁵. Other characteristics of protection in these RhCMV/SIV vector-vaccinated female RM were identical to those previously reported for RhCMV/SIV vector-mediated protection against IR challenge⁵, including development of *de novo* SIVvif-specific CD8+ T cell responses, lack of an anamnestic boost of the vaccine-elicited SIV-specific CD4+ or CD8+ T cells, lack of SIVenv seroconversion, and lack of CD4+ T cell depletion at mucosal effector sites (Fig. 2b; Suppl. Figs. 9, 11, 12).

To determine whether SIV infection spread from the cervical/vaginal mucosa in the 9 RhCMV/SIV vector-protected female RM, we biopsied BM, peripheral LN (axillary/inguinal) and small intestinal mucosa for nested quantitative RT-PCR/PCR analysis at 5, 9, 17 and >30 weeks post-infection. Strikingly, in the first 9 weeks of infection, 5 of these 9 RM manifested levels of SIV RNA in BM comparable to levels seen in uncontrolled SIV infection, but, whereas in uncontrolled infection SIV RNA levels were similarly high in peripheral blood mononuclear cells (PBMC), LNs and intestinal mucosa, SIV RNA was either not detected or detected only at very low levels in these sites in the RhCMV/SIV vector-protected RM (Fig. 2c). Moreover, in contrast to uncontrolled infection, SIV DNA was inconsistently detected in the samples from the RhCMV/SIV vector-protected RM, and by 40 weeks post-infection all 9 of the RhCMV/SIV vector-protected RM had at least one sample set in which both SIV RNA and DNA were below the level of detection. In 8 of these RM (excluding Rh20363, see below), all samples obtained subsequent to 30 weeks post-infection showed SIV RNA and DNA below the level of detection, with the exception of 1 PBMC sample with low-level SIV RNA (454 c. eq./10⁸ cells). The differences in the frequency of SIV detection in samples obtained at 5, 9 and 17 weeks vs. >30 weeks post-infection from these 8 RM were highly significant ($p = 0.002$ for all samples, $p = 0.0006$ for BM by two-sided Wilcoxon Rank Sum tests).

The ability to detect tissue-associated SIV early, but not late, after infection in these 8 stably protected female RM, particularly in BM, is consistent with initial spread and subsequent control and progressive clearance of SIV, and in keeping with this, the frequencies of circulating SIVvif-specific T cells, which are elicited and maintained by antigen derived from SIV infection (rather than the vaccine), progressively declined in these RM until these responses were no longer detectable (Fig. 2b; Suppl. Fig. 11). However, despite having no detectable SIV RNA or DNA in PBMC and tissue samples at week 17 and declining SIVvif-specific T cell responses, one animal (Rh20363) showed the emergence of low-level productive SIV infection at week 31 post-infection (Fig. 2a). The boosting of SIV-specific CD4+ and CD8+ T cell responses (Fig. 2b; Suppl. Fig. 11), including *de novo* CD8+ T cell responses to canonical *Mamu-A*01*-restricted SIV epitopes (Suppl. Fig. 13), the appearance

of cell-associated RNA and DNA in subsequent PBMC, LN and intestinal samples (Fig. 2c), and the induction of increased plasma and PBMC-associated SIV loads with experimental *in vivo* CD8+ cell depletion (Suppl. Fig. 14) indicates that this RM spontaneously converted from a unique state of stringent viral containment with little or no ongoing viral replication to a different state characterized by ongoing low-level SIV replication (consistent with conventional “elite” immunologic control). In keeping with this, sequence analysis of the breakthrough virus 3 weeks after initial viral rebound showed little sequence evolution from the initial SIVmac239 sequence except, notably, a putative escape mutation in the Tat-SL8 epitope sequence, consistent with early escape from the Tat-SL8-specific T cell responses that developed after viral rebound at week 31 (Suppl. Figs. 13, 15). Given the enormous breadth of RhCMV/SIV vector-elicited CD8+ T cell responses¹⁰, this limited sequence evolution suggests that the loss of aviremic control in Rh20363 was more likely due to inadequate immune surveillance of residual infection than mutational escape. Experimental CD8+ cell depletion was also performed on 3 RhCMV/SIV vector-protected female RM that retained aviremic control, and in keeping with previous analysis of CD8+ lymphocyte depletion of RhCMV/SIV vector-vaccinated male RM protected after IR challenge^{5,9}, this treatment did not induce detectable plasma viremia (Suppl. Fig. 14). However, one of these RM (Rh21176) transiently manifested unequivocal detection of SIV RNA (10/10 replicates +) and replication competent SIV (7 of 20 co-cultures +) in LN at day 10 post-depletion, demonstrating the presence of at least local, very low level residual SIV infection in this RM after 52 weeks of stringent control. In contrast to Rh20363, Rh21176 maintained aviremic control indicating that this RM's immune system either controlled or eliminated residual foci of SIV replication.

The finding that RhCMV/SIV vector-protected RM are able to control hematogenous SIV dissemination after both IR and IVag challenge suggested that the immune responses elicited by these vectors might provide protection even when mucosal surfaces are bypassed. To assess this possibility, we challenged 6 RhCMV/SIV-vaccinated RM with low dose, intravenous (IV) SIVmac239, and found that 2 of these 6 RM manifested the same pattern of control observed after mucosal challenge – a transient, low-level viremia associated with the development of SIVvif-specific T cell response, and detection of SIV RNA in BM (high level) and/or PBMC (low level) early, but not late, after infection (Suppl. Fig. 16). Taken together, these data indicate that 1) RhCMV/SIV vector-elicited immune responses can mediate protection regardless of the route of SIV challenge, 2) viral control is both local and systemic, and 3) replication-competent SIV can persist in multiple sites for weeks to months in protected RM (even when aviremic), but appears to decline over time.

To determine the ultimate fate of residual SIV in RhCMV/SIV vector-protected RM, we followed a total of 10 protected RM for 68–180 weeks post-infection (Fig. 3a,b). In all these RM, plasma viral blips became increasingly infrequent over time, with no blips observed after 70 weeks. The frequency of the SIV infection-dependent, SIVvif-specific CD8+ T cells in blood also progressively declined in all RM until these responses were no longer detectable (Suppl. Fig. 17). In contrast to the SIVvif-specific CD8+ T cell responses, the SIV-specific CD8+ T cell responses elicited by the RhCMV/SIV vectors remained stable, including high frequencies of CD8+ T cells capable of recognizing autologous SIV-infected

CD4⁺ T cells (Suppl. Fig. 18). Analysis of 6 of these medium- to long-term protected RM at necropsy, including one RM that was CD8⁺ cell-depleted 10 days prior to necropsy (Suppl. Fig. 19), confirmed the systemic loss of SIVvif-specific CD4⁺ and CD8⁺ T cells, and the maintenance of RhCMV vector-elicited, SIV-specific T cells (Suppl. Fig. 20). Most importantly, ultrasensitive, nested quantitative PCR/RT-PCR analysis of 54 tissues per RM (10 replicates per tissue, including extensive sampling of all tissues shown to contain SIV in the short-term RhCMV/SIV vector-protected RM) revealed extremely low to absent levels of SIV DNA and RNA that were indistinguishable from measurements in unchallenged RhCMV/SIV-vaccinated (SIV⁻) controls (Fig. 3c,d; Suppl. Figs. 2, 21; Suppl. Tables 1 and 3). Moreover, despite extensive sampling (>240 cultures per animal), no replication-competent SIV was isolated by co-culture analysis from the lymphoid tissues of these RM (Table 1). Finally, we asked whether the adoptive transfer of a total of 6×10^7 hemolymphoid cells (3×10^7 each peripheral blood leukocytes and LN cells, or 3×10^7 each BM leukocytes and spleen cells) from 3 SIV⁺ control RM (2 with ART-suppressed infection and 1 elite controller) and 5 long-term RhCMV/SIV vector-protected RM (including 1 RM tested before and after CD8⁺ cell depletion) would initiate infection in SIV-naïve RM. Remarkably, although cells from the SIV⁺ controls, including ART-suppressed RM, rapidly initiated SIV infection in the SIV-naïve recipients (manifested by the onset of SIV replication and induction of SIVvif-specific T cell responses), no evidence of SIV infection was observed in the SIV-naïve recipients receiving cells from the medium- and long-term RhCMV/SIV vector-protected RM (Fig. 3e; Suppl. Fig. 22). Taken together, these data provide strong evidence that after being unequivocally infected with SIV, these RhCMV/SIV vector-vaccinated RM cleared detectable infection, such that by all measured criteria (vif-specific T cell responses, extensive ultrasensitive PCR/RT-PCR and co-culture analysis, and adoptive transfer) these RM were indistinguishable from RhCMV/SIV vector-vaccinated controls that had never been exposed to SIV. Although we cannot rule out residual virus below our level of detectability, or in tissues not examined, these data strongly support progressive immune-mediated clearance of an established lentivirus infection, leading to a situation meeting criteria for a functional cure¹² and consistent with possible viral eradication.

In the past 5 years, the HIV/AIDS vaccine field has concluded that a prophylactic HIV/AIDS vaccine must prevent or eliminate HIV infection, as it is thought that any residual infection runs a high risk of eventual progression¹³. Our demonstration here that the virus-specific, effector memory T cells maintained by a persistent vector can shut down productive SIV infection, and by maintaining immune surveillance over time, functionally cure and possibly eradicate a highly pathogenic SIV infection, indicates that an effector memory T cell-targeted vaccine could (by itself, or combined with antibody-targeted approaches) provide meaningful long-term efficacy. Our results also suggest that an effector memory T cell-targeted vaccine might contribute to HIV cure strategies. Although the SIV reservoirs that initially develop in RhCMV/SIV vector-vaccinated controllers are smaller in size, and possibly different in character from HIV/SIV reservoirs in the setting of ART administration initiated in chronic infection, it is conceivable that the indefinitely persistent, unconventionally targeted¹⁰, viral-specific T cells elicited and maintained by CMV vectors – alone or in combination with agents designed to activate HIV gene expression^{1,2,12} – might

exert potent immune pressure on cells with any HIV protein expression (including expression of viral antigen by stochastically activated, latently infected cells) and thereby facilitate depletion of residual HIV reservoirs in patients on suppressive ART. It is also possible that these responses might stringently control recrudescence “rebound” infection after ART withdrawal in a manner analogous to their control of primary SIV infection in this study. In summary, the ability of CMV vectors to implement continuous, long-term, and potent anti-pathogen immune surveillance makes them promising candidates for vaccine strategies intended to prevent and cure HIV/AIDS, as well as other chronic/persistent infections.

FULL METHODS

Rhesus macaques

Ninety-nine purpose-bred male and female RM (*Macaca mulatta*) of Indian genetic background were used with the approval of the Oregon National Primate Research Center Animal Care and Use Committee, under the standards of the US National Institutes of Health Guide for the Care and Use of Laboratory Animals. These animals were specific-pathogen free (SPF) as defined by being free of cercopithecine herpesvirus 1, D-type simian retrovirus, simian T-lymphotrophic virus type 1, rhesus rhadinovirus, and *Mycobacterium tuberculosis*. MHC-1 genotyping for common *Mamu* alleles such as *Mamu-A*01/-A*02* and *-B*08/-B*17* was performed by sequence-specific priming PCR, as described¹⁶. The 99 RM include 15 RhCMV/SIV vector-vaccinated RM (7–10 years of age) with aviremic control of SIV infection (14 with SIVmac239, 1 with SIVmac251) after IR challenge (5 with short-term follow up; 10 with medium- to long-term follow up), 52 RM (4–19 years of age) vaccinated with RhCMV/SIV or control RhCMV vectors or left unvaccinated prior to SIVmac239 challenge (42 IVag, 10 IV), 12 SIV+ RM (5–12 years of age; 8 with progressive SIVmac239 infection, 1 with spontaneously controlled SIVmac239 infection, 3 with ART-suppressed SIVmac251 infection), and 20 SIV-naïve RM (4–14 years of age) used as negative controls (these include 4 RM vaccinated with RhCMV/SIV vectors) or as SIV– and RhCMV vector-naïve recipients in the adoptive transfer experiments. Early (<1 year) follow up of 8 of the RhCMV/SIV vector-vaccinated RM with long-term, aviremic control of SIV infection was previously reported⁵, with this study extending that follow-up from 1 to >3 years. RhCMV/gag, rev/tat/nef, env and pol-1 and pol-2 vectors were administered subcutaneously at a dose of 5×10^6 plaque forming units per vector. The control Ag-expressing RhCMV vector was used at a total dose of 2.5×10^6 plaque forming units to match the total dose of the RhCMV/SIV vectors. RM were vaccinated twice with RhCMV vectors, 14 weeks apart. All SIV challenges (IR, IVag, IV) used a repeated limiting dose protocol using dosing designed to require >1 challenge for infection of >60% of challenged RM, and to infect all or nearly all challenged RM with 10 (weekly) challenges for IR or IVag inoculation (300 focus forming units) and 3 (every 3rd week) challenges for IV inoculation (0.2 focus-forming units). RM were considered SIV-infected (and challenge discontinued) with the onset of plasma viral load ≥ 30 c. eq./ml and the *de novo* development of CD4+ and CD8+ T cell responses to SIVvif, an SIV Ag not included in the RhCMV/SIV vectors. RM were considered controllers if plasma viral load became undetectable (<30 c. eq./ml) within 2 weeks of the initial positive plasma viral load and was then maintained

below threshold for 3 consecutive determinations. RM with progressive SIV infection were followed for 20 weeks post-infection, or if progression was rapid, until the onset of AIDS. ART consisted of 2 reverse transcriptase inhibitors (20 mg/day Tenofovir, 50 mg/day Emtricitabine), an integrase inhibitor (240 mg/day Raltegravir) and a protease inhibitor (600 mg twice daily Darunavir boosted with 100 mg twice daily Ritonavir). Selected RM were depleted of CD8⁺ lymphocytes by administration of 10, 5, 5, and 5 mg per kg body weight of the CD8 α monoclonal antibody (mAb) M-T807R1, a modified version of the cM-T807 humanized anti-CD8 mAb with rhesus constant and variable framework regions (<http://nhpreagents.bidmc.harvard.edu>), administered on days 0, 3, 7 and 10, respectively¹⁴. Tissues obtained by biopsy or at necropsy were processed for mononuclear cell preparation, virologic, and/or immunohistologic analysis as previously described^{5,17}. For adoptive transfer experiments, freshly obtained peripheral blood and BM buffy coats were prepared by centrifugation (400xg for 20 minutes). These buffy coats and/or freshly obtained whole LN cell or splenocyte preparations were washed 3 times in saline prior to IV infusion with each RM receiving 3×10^7 peripheral blood leukocytes + 3×10^7 LN cells (or in 1 RM, 3×10^7 BM leukocytes + 3×10^7 splenocytes) over 1 hour.

Vectors and viruses

The construction and characterization of the strain 68-1-derived RhCMV/SIV vectors, including RhCMV(gag), RhCMV(rtn), RhCMV(env) and RhCMV(pol-1) and RhCMV(pol-2), has been previously described^{5,9}. A control RhCMV vector expressing an *M. tuberculosis* Ag85B-ESAT6 fusion protein under the control of the EF1- α promoter was constructed with the same E/T recombination approach and RhCMV (68-1) bacterial artificial chromosome (BAC) used for RhCMV/SIV construction⁹. RhCMV vector stocks were titered using primary rhesus fibroblasts in a TCID₅₀ assay. The pathogenic SIV challenge stocks used in these experiments were generated by expanding the SIVmac239 clone (or SIVmac251 swarm) in RM PBMC, and were titered using the sMAGI cell assay.

Viral detection assays

Plasma viral loads were determined by quantitative RT-PCR as previously described^{18,19}. Ultrasensitive determinations of plasma viral loads at necropsy were achieved by concentrating virus from the larger volumes of material available by ultracentrifugation (#6041 10 mL tubes and #4018 crown assembly, Seton Scientific; T1270 rotor, Thermo-Sorvall Scientific) at $170,000 \times g$ for 30 min prior to processing RNA. Reactions were also run in triplicate and followed the analysis recommendations in Palmer, *et al.*²⁰ permitting per reaction determinations of 1 copy (2 of 3 positive amplifications) and threshold sensitivities correspondingly lower, dependent on the amount of plasma input. Plasma viral sequencing of Rh20363 post-rebound was performed by synthesis of cDNA with SIV gene specific primers followed by sequencing using the single genome amplification strategy²¹ (Genbank accession #s KF439057, KF439058, KF439059). Quantitative assessment of SIV DNA and RNA in isolated cells and tissues were determined by the quantitative hybrid real-time/digital RT-PCR and PCR assays, essentially as previously described⁵, but with modifications to allow more efficient processing of samples larger than ~100 mg and to increase sample throughput. With respect to the former, the large tissue samples were directly disrupted in TriReagent® (Molecular Research Center, Inc.) utilizing two 7/16"

stainless steel balls over 10–15 stainless steel hex nuts (5.5 mm wide) as grinding media, rather than first attempting to cryogenically pulverize the tissue. With respect to the latter, the RT-PCR and PCR assay conditions were also modified to reduce reaction volumes to allow use of 384-well plates. The cDNA reactions were reduced to 15 μ l comprised of 10 μ l sample plus 5 μ l concentrated reaction cocktail and contained 2 mM SIVnestR01 primer, 10 units RNAsin, and 50 units MoMLV reverse transcriptase (Promega). The cDNA synthesis stage of the thermal profile was optimal for MoMLV reverse transcription at 37°C for 60 min, as opposed to 42°C for 40 min. The RT-PCR pre-amplification reactions were 25 μ l in volume with 1.25 units of PlatinumTaq polymerase (Life Technologies, Inc.) and 2.5 μ l of this reaction was transferred to 20 μ l of real-time PCR reaction mix with 1 unit of PlatinumTaq polymerase. For DNA determinations, the preamplification reactions were 20 μ l in volume, comprised of 10 μ l sample and 10 μ l reaction cocktail; 2 μ l of this “nested” reaction was transferred to 20 μ l of real-time PCR reaction mix. As previously described, for both RNA and DNA determinations, 12 replicate reactions were tested per sample including a spike of RNA or DNA internal control sequence standard in two of the 12 reactions to assess overall amplification efficiency and assess potential inhibition of the PCR or RT-PCR. The amount of DNA or RNA standard added to replicate reactions to monitor inhibition and PCR performance was typically 10 to 100 copies, depending on the anticipated level of SIV sequences present. Samples showing greater than a 5 cycle shift in amplification of the spiked standard, compared to amplification in the absence of specimen nucleic acid, corresponding to less than 74% overall amplification efficiency, were diluted and re-assayed. Quantitative determinations for samples showing amplification in all replicates were derived directly with reference to a standard curve. Quantitative determinations for samples showing fewer than 10 positive amplifications in replicates were derived from the frequency of positive amplifications, corresponding to the presence of at least one target copy in a reaction, according to a Poisson distribution of a given median copy number per reaction. To avoid false positives in biopsy material, where the specimen size and total number of specimens is limited, we required a minimum of 2 positive reactions out of 10 for a sample to be considered positive. The presence of inducible, replication-competent SIV in mononuclear cell preparations derived from different tissue sites at necropsy was detected by co-cultivation of 2.5×10^5 unfractionated cells from each tissue with 2×10^5 CEMx174 cells (x 20 replicates per tissue, cell numbers permitting; CEMx174 cells obtained from NIH AIDS Research & Reference Reagent Program)¹⁵. After 18 days, each culture was stained for CD3, CD4 and intracellular SIVgag-p27 (mAb 55-2F12) with positive cultures based on 0.5% CEMx174 cells with intracellular SIVgag expression over background by flow cytometry.

Immunologic assays

SIV-specific CD4⁺ and CD8⁺ T cell responses were measured in blood and tissues by flow cytometric intracellular cytokine analysis, as previously described in detail^{5,9}. To determine T cell responses to SIV peptide mixes or individual peptides, mononuclear cells were incubated with mixes of overlapping 15mer peptides comprising SIV proteins or individual epitopic 8-10mer peptides (with every individual peptide always at 2 μ g/ml) and the co-stimulatory molecules CD28 and CD49d (BD Biosciences) for 1 hour, followed by addition of Brefeldin A (Sigma-Aldrich) for an additional 8 hrs. Co-stimulation without antigen

served as a background control. To determine responses to autologous SIV-infected cells, SIV⁺ and SIV⁻ target cells were produced by spinoculating (or not spinoculating) activated CD4⁺ T cells with sucrose-purified SIVmac239, followed by culturing the cells for 4 days and then purifying the CD4⁺ cells with CD4 microbeads and LS columns (Miltenyi Biotec), as described²². These cell preparations were >95% CD4⁺ T cells and the SIV-infected preparations were >50% SIV⁺ following enrichment. SIV⁺ vs. SIV⁻ T cells were then incubated with microbead-purified CD8⁺ T cells at an effector:target ratio of 40:1 under the same conditions used for peptide-specific flow cytometric intracellular cytokine analysis. Following incubation, stimulated cells were stored at 4°C until staining with combinations of fluorochrome-conjugated mAbs including: SP34-2 (CD3; Pacific Blue, PerCP-Cy5.5), L200 (CD4; AmCyan), SK-1 (CD8 α ; APC, PerCP-Cy5.5), CD28.2 (CD28; PE, PE-TexasRed), DX2 (CD95; APC, PE), 15053 (CCR7; Pacific Blue), B56 (Ki-67; FITC), MAB11 (TNF- α ; APC, FITC, PE), B27 (IFN- γ ; APC, FITC), and FN50 (CD69; PE, PE-TexasRed). Data was collected on an LSR-II (BD Biosciences). Analysis was performed using FlowJo software (Tree Star). In all analyses, gating on the lymphocyte population was followed by the separation of the CD3⁺ T cell subset and progressive gating on CD4⁺ and CD8⁺ T cell subsets. Antigen-responding cells in both CD4⁺ and CD8⁺ T cell populations were determined by their intracellular expression of CD69 and either or both of the IFN- γ and TNF cytokines. After subtracting background, the raw response frequencies were memory corrected, as previously described^{5,9}. In selected experiments, cells responding to SIV peptides by production of either or both of IFN- γ and TNF were directly phenotyped with respect to the memory markers CD28 and CCR7^{5,9}. Titres of SIVenv-specific Abs were determined by neutralization of tissue culture-adapted SIVmac251 using a luciferase reporter gene assay²³.

Immunohistology

Immunohistochemistry was performed using a biotin-free polymer approach (Golden Bridge International, Inc.) on 5 μ m tissue sections mounted on glass slides, which were dewaxed and rehydrated with double-distilled H₂O. Heat induced epitope retrieval (HIER) was performed by heating sections in 0.01% citraconic anhydride containing 0.05% Tween-20 in a pressure cooker set at 122–125°C for 30 sec. Slides were incubated with blocking buffer (TBS with 0.05% Tween-20 and 0.5% casein) for 10 min. For APOBEC3G, slides were incubated with rabbit anti-APOBEC3G (1:100; Sigma HPA001812) diluted in blocking buffer overnight at 4°C. Slides were washed in 1X TBS with 0.05% Tween-20, endogenous peroxidases blocked using 1.5% (v/v) H₂O₂ in TBS (pH 7.4) for 10 min., incubated with Rabbit Polink-2 HRP and developed with ImpactTM DAB (3,3'-diaminobenzidine; Vector Laboratories). For ISG15 staining, after the HIER step, the slides were loaded on an IntelliPATH autostainer (Biocare Medical) and stained with optimal conditions determined empirically that consisted of a blocking step using blocking buffer (TBS with 0.05% Tween-20 and 0.5% casein) for 10 min. and an endogenous peroxidase block using 1.5% (v/v) H₂O₂ in TBS (pH 7.4) for 10 min. Rabbit anti-ISG (1:250; Sigma HPA004627) was diluted in blocking buffer and incubated for 1h at room temperature. Tissue sections were washed and developed using the Rabbit Polink-1 HRP staining system (Golden Bridge International, Inc.) according to manufacturer's recommendations. Sections were developed with ImpactTM DAB (Vector Laboratories). All slides were washed in H₂O, counterstained with hematoxylin, mounted in

Permount (Fisher Scientific), and scanned at high magnification (x200) using the ScanScope CS System (Aperio Technologies) yielding high-resolution data from the entire tissue section. Representative regions of interest (500 mm²) were identified and high-resolution images extracted from these whole-tissue scans. The percent area of the T cell zone that stained for APOBEC3G and ISG15 were quantified using Photoshop CS5 and Fovea tools.

Statistical analysis

The RM used in the vaccine efficacy analysis were randomly assigned to vaccine groups with randomization stratified to balance groups for expression of protective MHC alleles. All reported experiments were conducted once and are reported fully. The criteria for categorizing post-challenge RM into “protected” vs. “unprotected” groups were established previously⁵. Experimenters were not explicitly blinded to the treatment assignments of the RM, nor were the analyses conducted by blinded investigators. All statistical analyses were conducted using nonparametric and model-independent analysis procedures either for the main analysis or as a sensitivity analysis, and in every sensitivity analysis the result was qualitatively consistent with the main analysis. No tests depended on an assumption of equal variance across compared groups. The only exceptions were the time series analyses, which were conducted with two model-based (regression) approaches; the residuals of these analyses were evaluated and found to be consistent with homoscedasticity and normality requirements, and the results were consistent across approaches. For comparisons of continuous-valued data from independent samples, we applied bivariate Mann-Whitney U tests²⁴, also known as Wilcoxon Rank Sum tests. For comparisons of dichotomous values across groups, we applied Fisher’s exact tests²⁵. We estimated confidence bounds for binomial proportions using the Wilson score method, as described in Agresti and Coull²⁶. We compared group means of positivity frequencies for which we have repeated binary measures on individual RM using mixed effects logistic regression (with individual RM mean deviations from group means modeled as a normally-distributed random effect). We compared confidence intervals for RM groups to confidence intervals for individual RM (from other groups) by directly determining overlap of the intervals (and we used the estimated random effect variance and estimated group means to conduct z-tests in sensitivity analyses, which yielded consistent results). We compared Kaplan-Meier curves using the logrank test²⁷. We conducted time series analyses using standard linear regression with time as the primary predictor, and we used Gaussian first-order autoregressive process models in sensitivity analyses, which yielded consistent results. All tests were conducted as two-tailed tests with a type-I error rate of 5%. We used the R statistical computing language²⁸ for all statistical analyses.

Supplementary Material

Refer to Web version on PubMed Central for supplementary material.

Acknowledgments

This work was supported by the AIDS Vaccine Research in Nonhuman Primates Consortium of the National Institute of Allergy and Infectious Diseases (NIAID; U19 AI095985), as well as other NIAID grants (RO1 AI060392; R37 AI054292, P01 AI094417, U19 AI096109); the Bill & Melinda Gates Foundation-supported Collaboration for AIDS Vaccine Discovery (CAVD); the International AIDS Vaccine Initiative (IAVI) and its

donors, particularly the United States Agency for International Development (USAID); the National Center for Research Resources (P51 OD011092); and the National Cancer Institute (contract HHSN261200800001E). We thank A. Sylwester, A. Okoye, C. Kahl, S. Hagen, R. Lum, Y. Fukazawa, S. Shiigi, and L. Boshears for technical or administrative assistance; C. Miller, N. Miller, and T. Friedrich for provision of SIV stocks, K. Reimann for provision of the CD8-depleting mAb; D. Watkins for MHC typing; D. Montefiori for nAb assays; and A. Townsend for figure preparation.

References

1. Chun TW, Fauci AS. HIV reservoirs: Pathogenesis and obstacles to viral eradication and cure. *AIDS*. 2012; 26:1261–1268. [PubMed: 22472858]
2. Lewin SR, Evans VA, Elliott JH, Spire B, Chomont N. Finding a cure for HIV: Will it ever be achievable? *J Int AIDS Soc*. 2011; 14:4. [PubMed: 21255462]
3. Deeks SG, Walker BD. Human immunodeficiency virus controllers: Mechanisms of durable virus control in the absence of antiretroviral therapy. *Immunity*. 2007; 27:406–416. [PubMed: 17892849]
4. Picker LJ, Hansen SG, Lifson JD. New paradigms for HIV/AIDS vaccine development. *Annu Rev Med*. 2012; 63:95–111. [PubMed: 21942424]
5. Hansen SG, et al. Profound early control of highly pathogenic SIV by an effector memory T-cell vaccine. *Nature*. 2011; 473:523–527. [PubMed: 21562493]
6. Haase AT. Early events in sexual transmission of HIV and SIV and opportunities for interventions. *Annu Rev Med*. 2011; 62:127–139. [PubMed: 21054171]
7. Lifson JD, et al. Containment of simian immunodeficiency virus infection: cellular immune responses and protection from rechallenge following transient postinoculation antiretroviral treatment. *J Virol*. 2000; 74:2584–2593. [PubMed: 10684272]
8. Saez-Cirion A, et al. Post-Treatment HIV-1 Controllers with a Long-Term Virological Remission after the Interruption of Early Initiated Antiretroviral Therapy ANRS VISCONTI Study. *PLoS Pathogens*. 2013; 9:e1003211. [PubMed: 23516360]
9. Hansen SG, et al. Effector memory T cell responses are associated with protection of rhesus monkeys from mucosal simian immunodeficiency virus challenge. *Nat Med*. 2009; 15:293–299. [PubMed: 19219024]
10. Hansen SG, et al. Cytomegalovirus vectors violate CD8+ T cell epitope recognition paradigms. *Science*. 2013; 340:1237874.10.1126/science.1237874 [PubMed: 23704576]
11. Ribeiro Dos Santos P, et al. Rapid dissemination of SIV follows multisite entry after rectal inoculation. *PLoS One*. 2011; 6:e19493. [PubMed: 21573012]
12. Deeks SG, et al. Towards an HIV cure: a global scientific strategy. *Nat Rev Immunol*. 2012; 12:607–614. [PubMed: 22814509]
13. Burton DR, et al. A Blueprint for HIV Vaccine Discovery. *Cell Host & Microbe*. 2012; 12:396–407. [PubMed: 23084910]
14. Okoye A, et al. Profound CD4+/CCR5+ T cell expansion is induced by CD8+ lymphocyte depletion but does not account for accelerated SIV pathogenesis. *J Exp Med*. 2009; 206:1575–1588. [PubMed: 19546246]
15. Shen A, et al. Novel pathway for induction of latent virus from resting CD4(+) T cells in the simian immunodeficiency virus/macaque model of human immunodeficiency virus type 1 latency. *J Virol*. 2007; 81:1660–1670. [PubMed: 17151130]
16. Loffredo JT, et al. *Mamu-B*08*-positive macaques control simian immunodeficiency virus replication. *J Virol*. 2007; 81:8827–8832. [PubMed: 17537848]
17. Tabb B, et al. Reduced inflammation and lymphoid tissue immunopathology in rhesus macaques receiving anti-tumor necrosis factor treatment during primary simian immunodeficiency virus infection. *J Infect Dis*. 2013; 207:880–892. [PubMed: 23087435]
18. Cline AN, Bess JW, Piatak M Jr, Lifson JD. Highly sensitive SIV plasma viral load assay: practical considerations, realistic performance expectations, and application to reverse engineering of vaccines for AIDS. *J Med Primatol*. 2005; 34:303–312. [PubMed: 16128925]
19. Venneti S, et al. Longitudinal in vivo positron emission tomography imaging of infected and activated brain macrophages in a macaque model of human immunodeficiency virus encephalitis

- correlates with central and peripheral markers of encephalitis and areas of synaptic degeneration. *Am J Pathol.* 2008; 172:1603–1616. [PubMed: 18467697]
20. Palmer S, et al. New real-time reverse transcriptase-initiated PCR assay with single-copy sensitivity for human immunodeficiency virus type 1 RNA in plasma. *J Clin Microbiol.* 2003; 41:4531–4536. [PubMed: 14532178]
 21. Keele BF, et al. Low-dose rectal inoculation of rhesus macaques by SIVsmE660 or SIVmac251 recapitulates human mucosal infection by HIV-1. *J Exp Med.* 2009; 206:1117–1134. [PubMed: 19414559]
 22. Sacha JB, Watkins DI. Synchronous infection of SIV and HIV *in vitro* for virology, immunology and vaccine-related studies. *Nat Protoc.* 2010; 5:239–246. [PubMed: 20134424]
 23. Montefiori DC. Evaluating neutralizing antibodies against HIV, SIV, and SHIV in luciferase reporter gene assays. *Curr Protoc Immunol.* 2005; Chapter 12(Unit 12.11)
 24. Wolfe, DA.; Hollander, M. *Nonparametric Statistical Methods.* Wiley; New York: 1973.
 25. Fisher RA. The logic of inductive inference. *Journal of the Royal Statistical Society Series A.* 1935; 98:39–54.
 26. Agresti A, Coull BA. Approximate is better than “exact” for interval estimation of binomial proportions. *American Statistician.* 1998; 52:119–126.
 27. Harrington DP, Fleming TR. A class of rank test procedures for censored survival data. *Biometrika.* 1982; 69:553–566.
 28. R Development Core Team. *R, A Language and Environment for Statistical Computing.* 2011. <http://www.R-project.org>
 29. Allen TM, et al. Tat-specific cytotoxic T lymphocytes select for SIV escape variants during resolution of primary viraemia. *Nature.* 2000; 407:386–390. [PubMed: 11014195]
 30. Goulder PJ, Watkins DI. Impact of MHC class I diversity on immune control of immunodeficiency virus replication. *Nat Rev Immunol.* 2008; 8:619–630. [PubMed: 18617886]

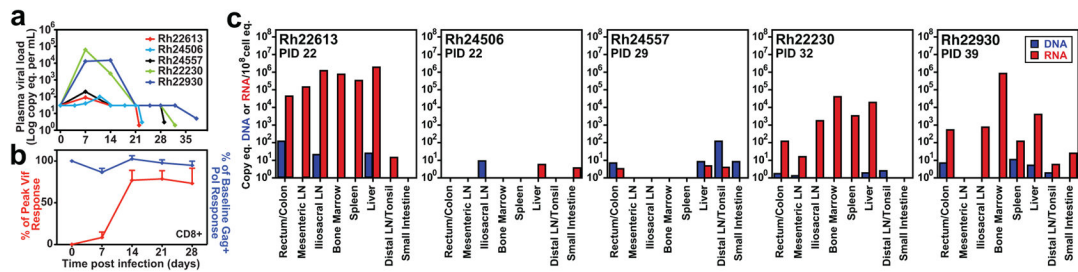


Figure 1. Virologic analysis of early RhCMV/SIV vector-mediated protection

a, Plasma viral load (pvl) profiles of 5 RhCMV/SIV vector-vaccinated RM with complete control of viremia following IR SIVmac239 challenge. All 5 RM controlled viremia to below the 30 c. eq./ml limit of quantification for the standard pvl assay used for all pre-necropsy samples, and to below the 1–5 c. eq./ml limit of detection for the ultrasensitive pvl assay used on necropsy samples (individual detection limits for each terminal sample shown). **b**, Frequencies of peripheral blood memory CD8+ T cells specific for SIV proteins that were (Gag + Pol) or were not (Vif) included in the RhCMV/SIV vectors, shown before and after the onset of the controlled SIV infection. The response frequencies (plotted as mean \pm SEM) were normalized to the response frequencies immediately prior to SIV infection for the vaccine-elicited SIVgag- and SIVpol-specific responses, and to the peak frequencies following SIV infection for the *de novo* SIVvif-specific responses. **c**, Analysis of tissue-associated SIV DNA and RNA in the 5 RhCMV/SIV vector-protected RM at necropsy using ultrasensitive quantitative PCR/RT-PCR (PID, post-infection day).

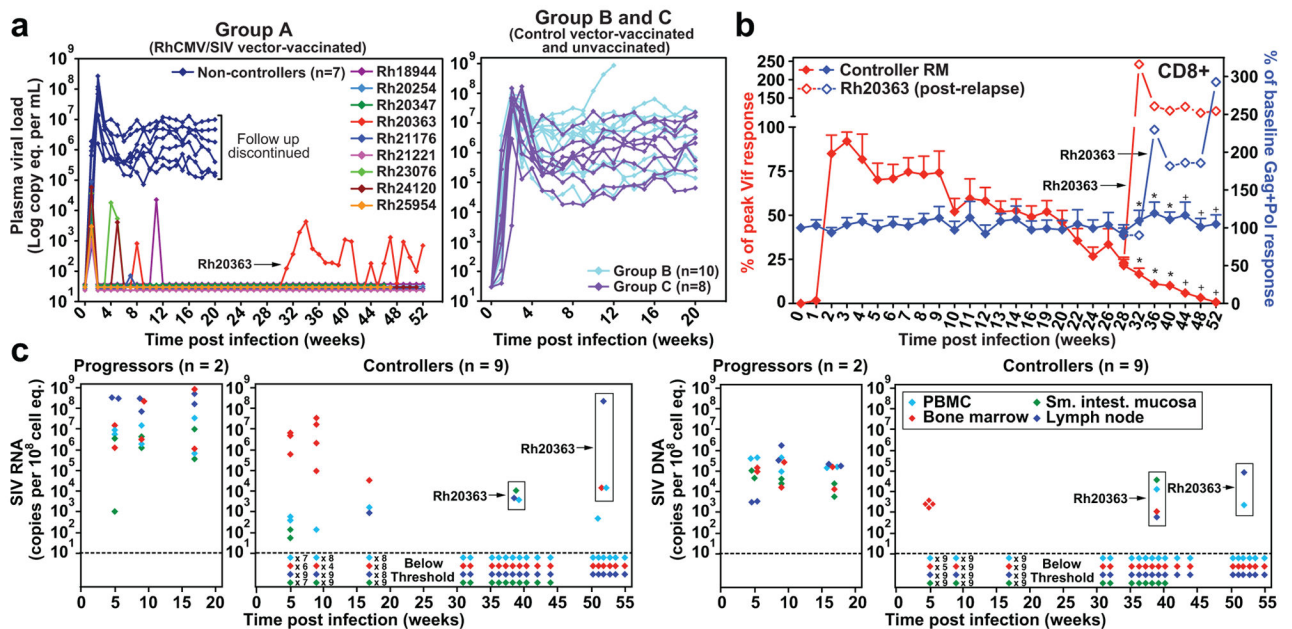


Figure 2. Longitudinal analysis of RhCMV/SIV vector-mediated protection after IVag challenge
a, Plasma viral load profiles of Groups A–C RM after infection by repeated, limiting dose, IVag SIVmac239 challenge, with the day of infection defined as the challenge prior to the first above-threshold plasma viral load. The fraction of infected RM that met controller criteria (see Full Methods) in Group A (9 of 16) vs. Groups B and C (0 of 18) was significantly different ($p = 0.0002$) by two-sided Fisher’s exact test. Note that Rh20363 initially manifested aviremic protection, but then relapsed with productive, albeit controlled, infection at week 31 post-infection. **b**, Mean (\pm SEM) frequencies of peripheral blood memory CD8+ T cells specific for SIV proteins that were (Gag + Pol) or were not (Vif) included in the RhCMV/SIV vectors, measured before and after the onset of SIV infection in the 9 Group A RM with initial aviremic control (response frequencies normalized as described in Fig. 1b). The asterisk indicates $n = 8$ (minus Rh20363 post-relapse) and the plus sign indicates $n = 7$ (minus Rh20363 and Rh20347, the latter used in the CD8+ cell depletion study described in Suppl. Fig. 14). **c**, Quantification of tissue-associated SIV RNA (left panel) and DNA (right panel) in the designated longitudinal samples of the 9 Group A controllers vs. 2 representative viremic progressors. All sample types were analyzed at weeks 5, 9 and 17 in all RM. All sample types were analyzed a 4th time in all controller RM between post-infection weeks 30–40, and PBMC, BM and LN samples were analyzed a 5th time in 8 of 9 controller RM between post-infection weeks 42 and 55. Each symbol represents a single determination from the designated tissue, except when a multiplication factor is shown (e.g., x 7 indicates a total of 7 samples from different RM with below threshold measurements for that time point).

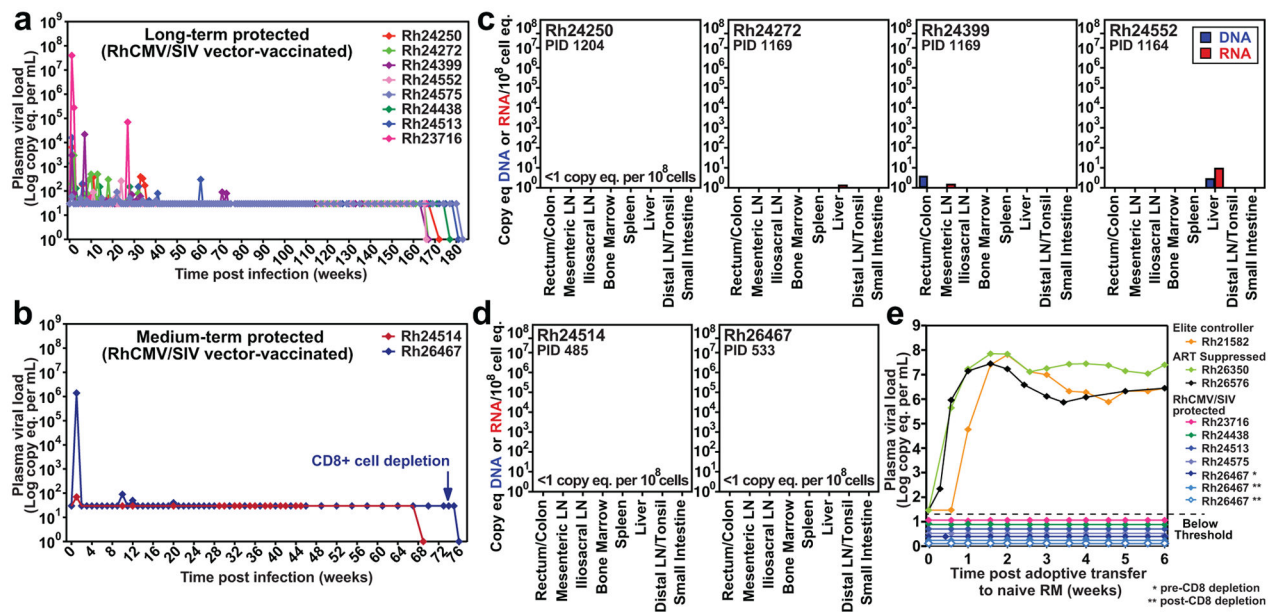


Figure 3. Virologic analysis of medium- to long-term RhCMV/SIV vector-mediated protection
a,b, Plasma viral load profiles of 10 RhCMV/SIV vector-vaccinated RM that controlled SIV infection after IR challenge (8 long-term; 2 medium-term). The limit of detection for all pre-terminal plasma viral load assays is 30 c. eq./ml; the limit of detection for the ultrasensitive assay used on the terminal sample of the study was 1 c. eq./ml. Note that one of the RM with medium-term protection (Rh26467) was CD8+ cell-depleted 10 days prior to the terminal sample. **c,d**, Quantification of tissue-associated SIV DNA and RNA in 4 long-term and 2 medium-term protected RhCMV/SIV-vaccinated RM studied at necropsy, including the CD8+ cell-depleted RM (Rh26467). **e**, Assessment of residual replication-competent, cell-associated SIV in medium- and long-term protected RM by adoptive transfer of 6×10^7 hemolymphoid cells (3×10^7 blood leukocytes and 3×10^7 LN cells or, in one transfer from Rh26467, represented by the open symbol, 3×10^7 BM leukocytes and 3×10^7 spleen cells) to SIV-naïve RM with SIV infection in the recipient RM delineated by plasma viral load. Cell transfers from RM with conventional elite SIV control and ART-suppressed SIV infection resulted in rapid onset of SIV infection in the recipient RM, but no SIV infection was observed in RM receiving cells from medium- to long-term RhCMV/SIV vector-protected RM (including Rh26467, analyzed both before and after CD8+ cell depletion).

Table 1

Detection of replication-competent SIV by inductive co-culture at necropsy (frequency of SIV+ cultures^{*})

| Animal | Progressor | Elite Controller | ART Suppressed | RhCMV/SIV vector-protected | | | | | | | | | | | |
|---|------------|------------------|----------------|----------------------------|-----------|-----------|-----------|-----------|----------------------|-----------|-----------|-----------|-----------|-----------|-----------|
| | | | | Early-term | | | | | Medium and long-term | | | | | | |
| | | | | Rh22613 | Rh24506 | Rh24557 | Rh22230 | Rh22930 | Rh24514 | Rh26467 | Rh24552 | Rh24272 | Rh24399 | Rh24250 | |
| Virus | SIVmac239 | SIVmac239 | SIVmac251 | SIVmac239 | SIVmac239 | SIVmac239 | SIVmac239 | SIVmac239 | SIVmac239 | SIVmac239 | SIVmac251 | SIVmac239 | SIVmac239 | SIVmac239 | SIVmac239 |
| Plasma SIV (copy eq./mL) | 110,000 | 510 | 11 | <2 | <3 | <3 | <2 | <5 | <1 | <1 | <1 | <1 | <1 | <1 | <1 |
| Duration of infection at necropsy (weeks) | 74 | 28 | 63** | 3 | 3 | 4 | 5 | 5 | 69 | 76 | 166 | 167 | 167 | 172 | |
| SIV+ cultures / Total cultures | | | | | | | | | | | | | | | |
| Distal lymph nodes | 80/80 | 32/80 | 4/49 | 0/80 | 0/80 | 0/80 | 0/60 | 1/100 | 0/80 | 0/80 | 0/80 | 0/60 | 0/80 | 0/58 | |
| Iliosacral lymph node | 40/40 | 9/40 | 0/40 | 2/40 | 1/40 | 2/40 | 3/40 | 1/40 | 0/40 | 0/40 | 0/40 | 0/40 | 0/40 | 0/40 | |
| Mesenteric lymph nodes | 80/80 | 2/80 | 3/80 | 1/80 | 0/80 | 0/80 | 2/80 | 1/60 | 0/80 | 0/80 | 0/80 | 0/60 | 0/60 | 0/65 | |
| Spleen | 40/40 | 1/40 | 5/40 | 2/40 | 1/40 | 2/40 | 1/40 | 1/40 | 0/40 | 0/40 | 0/40 | 0/40 | 0/40 | 0/40 | |
| Liver | ND | 0/20 | 2/19 | 1/40 | 0/20 | 2/20 | ND | 0/20 | 0/20 | 0/20 | 0/20 | 0/20 | 0/20 | 0/20 | |
| Bone Marrow | ND | 0/20 | 0/20 | ND | 1/20 | 2/20 | 1/20 | 0/20 | 0/16 | 0/13 | ND | 0/20 | 0/20 | 0/20 | |
| Total Positive | 240/240 | 44/280 | 14/248 | 6/280 | 3/280 | 8/280 | 7/240 | 4/280 | 0/276 | 0/273 | 0/260 | 0/240 | 0/260 | 0/243 | |
| 28/1360 | | | | | | | | | 0/1549 | | | | | | |
| <div style="display: flex; justify-content: space-around; align-items: center;"> p < 0.0001 Fisher's exact test </div> | | | | | | | | | | | | | | | |

* 250,000 cells per culture

** 24 weeks post ART initiation

ND = No Data

Author Manuscript

Author Manuscript

Author Manuscript

Author Manuscript